*Progress In Electromagnetics Research C, Vol. 120, 253–263, 2022*

# Model Predictive Control of Permanent Magnet Synchronous Motor Based on Parameter Identification and Dead Time Compensation

**Xin Liu, Yanfei Pan, Lin Wang, Jian Xu, Yilin Zhu*, and Zhongshu Li**

**Abstract**—A model predictive control method for permanent magnet synchronous motor based on parameter identification and dead time compensation is proposed to solve the problems of poor parameter robustness and large current errors. In this method, the prediction model is firstly established based on the mathematical model of the permanent magnet synchronous motor. After that, the current error caused by the parameter change in the prediction model and the current harmonics caused by the dead time effect are basically analyzed theoretically. Then, the adaptive linear neural network algorithm is proposed to identify the motor parameters and applied to the prediction model, and the harmonic components are filtered out using the adaptive linear neural network algorithm. The recursive least squares algorithm is used to quickly update the system weights to improve the dead time compensation control effect. Finally, the effectiveness and correctness of the proposed algorithm are verified on the experimental platform. The experimental results show that the predictive control method of permanent magnet synchronous motor model based on parameter identification and dead time compensation can effectively reduce the current error of the control system and accelerate the dynamic response of the speed.

## 1. INTRODUCTION

Permanent magnet synchronous motor (PMSM) has the characteristics of simple structure, reliable operation, small size, high power density, wide speed range, etc. It is widely used in electric vehicles, wind power generation, CNC machine tools, and other fields [1–5]. How to achieve PMSM high-performance drive control has been a hot topic in the field of motor control, and many studies have been conducted on it. The PMSM-based model predictive control (MPC) algorithm is one of them. The method inherits the idea of vector control and decomposes the motor current into two components $i_d$ and $i_q$ in the $d$- and $q$-axis rotation coordinate system. Therefore, the goal of MPC can be attributed to the high performance control of the $d$- and $q$-axis currents. Finite control set model predictive control (FCS-MPC) is characterized by fast dynamic response because no special modulator is required to control the ON and OFF states of power devices [6], and in addition, the method has the advantages of intuitive principle and flexible design. However, its drawbacks are also particularly prominent, as the control method is based on the motor model and is therefore highly parameter dependent. Model mismatch can lead to the degradation of control performance. In the control process, there are many factors of model mismatch, such as electrical parameter changes and dead time effects, which are among the main factors causing the degradation of model prediction control performance.

In order to improve the performance of MPC, many scholars have made in-depth research on MPC. In [7], a new type of current predictive control based on fuzzy algorithm is proposed. The algorithm can adjust the effect of compensation link in real time through weight coefficient according to the running state of motor and the mismatch of model parameters of controller, so that the control

*Received 1 April 2022, Accepted 23 May 2022, Scheduled 13 June 2022*
* Corresponding author: Yilin Zhu (yl.zhu.dy@gmail.com).
The authors are with the Jiangsu Changjiang Intelligent Manufacturing Research Institute Co, Ltd., Changzhou 213001, China.

system has strong parameter robustness. In [8], an improved model predictive current control method based on incremental model is proposed, which enhances the robustness of parameters by observing the inductance value. In [9], a new MPC method is proposed. In this method, the indirect reference vector strategy is used to avoid the problem of parameter sensitivity and improve the parameter robustness and current control accuracy of the system. In [10], a model free predictive current control based on super local model is proposed. The algorithm only uses the input and output of the system, so it has strong parameter robustness. In [11], a robust predictive current control strategy based on observer is proposed to estimate disturbance and current, so as to solve the problems of parameter mismatch, digital delay, and external disturbance in the system. In [12, 13], a predictive direct control method is proposed to solve the problems of large torque ripple, large flux ripple, and poor robustness in the control system. However, it also increases the complexity of the system.

In view of the above research results and the shortcomings of each scheme, an MPC method of PMSM based on parameter identification and dead time compensation (DTC) is proposed in this paper. In this method, firstly, the prediction model is established according to the mathematical model of PMSM, and then the current error caused by parameters change and current harmonics caused by dead time effect (DTE) in the prediction model are analyzed theoretically. Then, the adaptive linear neural network (ADALINE) algorithm is proposed to identify motor parameters, and the current harmonics are filtered using the ADALINE algorithm. The recursive least squares (RLS) algorithm quickly updates the algorithm weights so as to complete the DTC control. Finally, the effectiveness and correctness of the proposed algorithm are verified on the experimental platform.

This paper consists of five sections. In Section 2, a prediction model of a PMSM is developed, and the errors are analysed. In Section 3, the ADALINE-based method is proposed to identify motor parameters, and the ADALINE-based algorithm is used to filter out current harmonics and complete the DTC algorithm. In Section 4, the correctness and effectiveness of the MPC method based on parameter identification and DTC are verified on the experimental platform. Finally, the findings of this paper are summarized in Section 5.

## 2. FINITE CONTROL SET MODEL PREDICTIVE CONTROL MATHEMATICAL MODEL

### 2.1. Prediction Model and Cost Function

The process of realizing surface mounted PMSM (SPMSM) control by FCS-MPC can be briefly described as follows: under all possible inverter switching conditions, the predictive current of the next step can be obtained by the predictive model established according to the PMSM mathematical model. At the same time, the control target is evaluated through the cost function, and the switch state corresponding to the minimum value is selected from the evaluation results as the output of the next control state.

The stator voltage equation of PMSM in the $d$- and $q$-axis rotating coordinate system can be expressed as

$$\begin{cases} u_d = Ri_d + L_d \dfrac{\mathrm{d}i_d}{\mathrm{d}t} - \omega_{\mathrm{e}} L_q i_q \\ u_q = Ri_q + L_q \dfrac{\mathrm{d}i_q}{\mathrm{d}t} + \omega_{\mathrm{e}} L_d i_d + \omega_{\mathrm{e}} \lambda_f \end{cases} \tag{1}$$

where $i_d$ and $i_q$ are $d$- and $q$-axis stator currents, respectively; $R$ is the stator resistance; $\lambda_f$ is the flux linkage of permanent magnet; $\omega_e$ is the rotor electric angular velocity; $L_d$ and $L_q$ are $d$- and $q$-axis stator inductances, respectively; $L_d = L_q = L_s$ in an SPMSM; $u_d$ and $u_q$ are $d$- and $q$-axis stator voltages, respectively.

The above formula is discretized by the first-order Euler method and transformed into the expression of stator current, which can be expressed as

$$\begin{cases} i_d(k+1) = \left(1 - \dfrac{R}{L_s} T_s\right) i_d(k) + \omega_e(k) T_s i_q(k) + \frac{T_s}{L_s} u_d(k) \\ i_q(k+1) = -\omega_e(k) T_s i_d(k) + \left(1 - \dfrac{R}{L_s} T_s\right) i_q(k) + \dfrac{T_s}{L_s} u_q(k) - \dfrac{\omega_e(k) \lambda_f}{L_s} T_s \end{cases} \tag{2}$$

where $k$ in parentheses represents the sampled value at the $k$ moment; $(k+1)$ in parentheses represents the calculated value at $(k+1)$ moment; $T_s$ indicates the control cycle.

Further, the current expression at $k+2$ can be obtained.

$$\begin{cases} i_d(k+2) = \left(1 - \dfrac{R}{L_s}T_s\right) i_d(k+1) + \omega_e(k) T_s i_q(k+1) + \dfrac{T_s}{L_s} u_d(k+1) \\ i_q(k+2) = -\omega_e(k) T_s i_d(k+1) + \left(1 - \dfrac{R}{L_s}T_s\right) i_q(k+1) + \dfrac{T_s}{L_s} u_q(k+1) - \dfrac{\omega_e(k+1)\lambda_f}{L_s} T_s \end{cases} \tag{3}$$

where $(k+2)$ in parentheses represents the predicted value at the time of $(k+2)$. $u_d(k+1)$ and $u_q(k+1)$ can be calculated from the switch state and the actual angle of the motor. Because the control cycle is very short, the speed of the motor is constant during this period, i.e., $\omega_e(k+1) = \omega_e(k)$.

The specific calculation process of $u_d(k+1)$ and $u_q(k+1)$ is

$$\begin{cases} u_d(k+1) = u_\alpha(k)\cos\theta_e(k) + u_\beta(k)\sin\theta_e(k) \\ u_q(k+1) = -u_\alpha(k)\sin\theta_e(k) + u_\beta(k)\sin\theta_e(k) \end{cases} \tag{4}$$

where $u_\alpha$ and $u_\beta$ are obtained by phase voltage reconstruction and coordinate transformation.

In the traditional space vector pulse width modulation (SVPWM) or sine wave pulse width modulation (SPWM), the corresponding duty cycle is obtained by comparing the modulation wave with the carrier, and the MPC can output the switching state at the next time without modulator. For all possible switching states at $(k+2)$ time, $u_d(k+1)$, $u_q(k+1)$, $i_d(k+2)$, and $i_q(k+2)$ can be calculated from formulas (3) and (4). Based on the $d$- and $q$-axis command currents, the following cost function is used, and the switching state with the smallest value of the cost function is calculated to finally control the ON and OFF of the power device. The expression of the cost function is

$$J = \left[i_d^* - i_d(k+2)\right]^2 + \left[i_q^* - i_q(k+2)\right]^2 \tag{5}$$

It can be seen from the above formulas that whether the motor current can be accurately predicted is closely related to the accuracy of the model. There is an error between the nominal electrical parameters of the motor and the actual value, and the electrical parameters will change with the actual working conditions of the motor. Therefore, accurate parameters are needed in the process of model predictive control to improve the control performance.

## 2.2. Error Analysis

### *2.2.1. Parameters Mismatch*

Suppose that the inductance of the prediction model at time $k$ is $L_s(k)$; the theoretical inductance is $L_s$; the resistance at time $k$ is $R(k)$; and the theoretical resistance is $R$. Then the predicted current output of the prediction model is

$$\begin{cases} i_{d0}(k+1) = \left(1 - \dfrac{R(k)}{L_s(k)}T_s\right) i_d(k) + \omega_e(k) T_s i_q(k) + \dfrac{T_s}{L_s(k)} u_d(k) \\ i_{q0}(k+1) = -\omega_e(k) T_s i_d(k) + \left(1 - \dfrac{R(k)}{L_s(k)}T_s\right) i_q(k) + \dfrac{T_s}{L_s(k)} u_q(k) - \dfrac{\omega_e(k)\lambda_f(k)}{L_s(k)} T_s \end{cases} \tag{6}$$

After subtracting the predicted current value obtained from the theoretical parameters from the predicted current output in Eq. (6), Eq. (7) can be obtained.

$$\begin{cases} \Delta i_d = i_{d0}(k+1) - i_d(k+1) = A\left[(R\Delta L_s - L_s\Delta R) i_d(k) - \Delta L_s u_d(k)\right] \\ \Delta i_q = i_{q0}(k+1) - i_q(k+1) = A\left[(R\Delta L_s - L_s\Delta R) i_q(k) - \Delta L_s u_q(k) + (L_s\Delta\lambda_f - \lambda_f\Delta L_s)\omega_e(k)\right] \end{cases} \tag{7}$$

where $A = T_s/[L_s(k) \cdot L_s]$, $\Delta L_s = L_s(k) - L_s$, $\Delta R = R(k) - R$, $\Delta\lambda_f = \lambda_f(k) - \lambda_f$.

Current errors $\Delta i_d(k+1)$ and $\Delta i_q(k+1)$ are related to the parameter errors $\Delta L_s$, $\Delta R$ and $\Delta\lambda_f$. At the same time, these errors are also affected by the currents and voltages at time $k$.

*2.2.2. Dead Time Effect*

Usually six power devices are used to drive PMSM, but the ideal zero delay of power devices cannot be achieved in the ON-OFF processes. Therefore, the dead time must be introduced to avoid the short circuit caused by the simultaneous conduction of the upper and lower bridge arms in the power drive circuit. Fig. 1 shows the voltage waveform when dead time is introduced, and switching delay and voltage drop of power device are considered. The dotted line represents the ideal voltage waveform, and the solid line represents the actual voltage waveform. In Fig. 1, $T_{on}$, $T_r$, $T_f$, $T_d$, and $T_{\mathrm{PWM}}$ represent the on-time, rise time, fall time, dead time, and PWM control cycle, respectively. $u_{dc}$, $u_T$, and $u_D$ are dc bus voltage, power device voltage drop, and diode voltage drop, respectively.

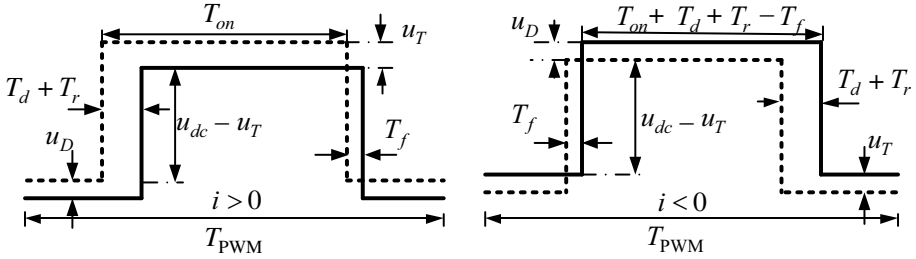


**Figure 1.** Ideal and actual voltage waveforms.

For SPMSM, the phase voltage change caused by the DTE can be transformed into voltage change in the $d$- and $q$-axis rotating coordinate system after Clarke transformation and Park transformation. After Fourier series expansion of the voltage, if only the main factors in the voltage harmonics are considered, the harmonics can be expressed as

$$\begin{cases} \Delta u_d = -\dfrac{48}{35\pi}\Delta u_{\mathrm{dead}} \sin(6\theta_e) \\ \Delta u_q = \dfrac{4}{\pi}\Delta u_{\mathrm{dead}} - \dfrac{8}{35\pi}\Delta u_{\mathrm{dead}} \cos(6\theta_e) \end{cases} \tag{8}$$

where $\Delta u_d$ and $\Delta u_q$ are the error voltages of $d$- and $q$-axis, respectively, and $\Delta u_{\mathrm{dead}}$ is the error voltage caused by DTE.

When the motor is regarded as resistive inductive load, the error currents can be expressed as

$$\begin{cases} \Delta i_d = \left(-\dfrac{4\Delta u_{\mathrm{dead}}}{\pi}\right) \cdot \dfrac{12\sin(6\omega_e t - \phi_6)}{35 Z_6} \\ \Delta i_q = \left(-\dfrac{4\Delta u_{\mathrm{dead}}}{\pi}\right) \cdot \left(-\dfrac{1}{R} + \dfrac{2\cos(6\omega_e t - \phi_6)}{35 Z_6}\right) \end{cases} \tag{9}$$

where the impedance and phase angle are $Z_6 = \sqrt{R^2 + (6\omega_e L_s)^2}$ and $\phi_6 = \tan^{-1}\frac{6\omega_e L_s}{R}$.

As can be seen from the above analysis, the deviation of parameters will cause the deviation of current prediction. At the same time, the introduction of dead time will cause the fluctuation of motor current. Therefore, on the basis of accurate identification of parameters, the DTE should be compensated effectively.

## 3. ERROR COMPENSATION CONTROL METHOD

Through the analysis of the previous section, the parameter mismatch and DTE will affect the performance of MPC. In order to identify the accurate motor parameters and compensate the DTE in real time, the parameter identification method based on ADALINE and the DTC control method based on ADALINE are proposed respectively.

### 3.1. Parameter Identification Method Based on ADALINE

When the motor is at rest, inject constant current of different amplitudes into the $d$-axis for many times. After calculation, the expression of stator resistance $R$ can be obtained [4]. The expression is

$$R = \frac{u_{d1} - u_{d0}}{i_{d1} - i_{d0}} \tag{10}$$

where $i_{d0}$ and $i_{d1}$ are the $d$-axis currents at different amplitudes; $u_{d0}$ and $u_{d1}$ are the $d$-axis voltages.

After the resistance identification is completed, the following current can be applied to the $d$-axis to identify the initial value of inductance.

$$i_d = I_{\mathrm{DC}} + I_{\mathrm{m1}} \cos(\omega t) \tag{11}$$

The impedance value $Z$ can be calculated by collecting the voltage response when the above current is applied. Then the initial value of inductance is calculated by the following formula.

$$L_s = \frac{\sqrt{Z^2 - R^2}}{\omega} \tag{12}$$

where $Z$ is the reactance; the value is $u_d/i_d$; $\omega$ is the frequency of the current injected into the $d$-axis.

Because the value of $\lambda_f$ is less affected by temperature, $i_d$ and $i_q$, according to (7), the value of $\lambda_f$ can be calculated through starting the motor with $i_d = 0$, running to a certain speed and running stably for a period of time.

$$\lambda_f = \frac{u_q - Ri_q}{\omega_e} \tag{13}$$

Considering the nonlinear factor of inverter, the mathematical model in steady state is

$$\begin{cases} u_d^* + \Delta u_{\mathrm{dead}} D_d = Ri_d - L_s \omega_e i_q \\ u_q^* + \Delta u_{\mathrm{dead}} D_q = Ri_q + L_s \omega_e i_d + \omega_e \lambda_f \end{cases} \tag{14}$$

$$\begin{cases} D_d = 2\left[\cos\theta_e \cdot \mathrm{sgn}(i_{as}) + \cos\left(\theta_e - \dfrac{2\pi}{3}\right) \cdot \mathrm{sgn}(i_{bs}) + \cos\left(\theta_e + \dfrac{2\pi}{3}\right) \cdot \mathrm{sgn}(i_{cs})\right] \\ D_q = 2\left[-\sin\theta_e \cdot \mathrm{sgn}(i_{as}) - \sin\left(\theta_e - \dfrac{2\pi}{3}\right) \cdot \mathrm{sgn}(i_{bs}) + \sin\left(\theta_e - \dfrac{\pi}{3}\right) \cdot \mathrm{sgn}(i_{cs})\right] \end{cases} \tag{15}$$

where sgn( ) represents a symbolic function.

The average value of (14) can be expressed as

$$\begin{cases} \bar{u}_d^* = R\bar{i}_d - L_s \bar{\omega}_e \bar{i}_q \\ \bar{u}_q^* = R\bar{i}_q + L_s \bar{\omega}_e \bar{i}_d + \bar{\omega}_e \lambda_f \end{cases} \tag{16}$$

where $\bar{u}_d^*$, $\bar{u}_q^*$, $\bar{i}_d^*$, $\bar{i}_q^*$, and $\bar{\omega}_e$ are the DC components of $u_d^*$, $u_q^*$, $i_d^*$, $i_q^*$,and $\omega_e$ after mean filtering. $D_d$ and $D_q$ are the 6th harmonics with a mean value of 0, so the DC components of $\Delta u_{\mathrm{dead}} D_d$ and $\Delta u_{\mathrm{dead}} D_q$ are 0.

In the stator voltage equation of $d$- and $q$-axis in (16), the values of $R$ and $\lambda_f$ are identified by the previous work. Therefore, there is no problem of under-rank and coupling for the identification of $L_s$, and the identification results will be more accurate. The value of $L_s$ is updated by the ADALINE algorithm which is single input and single output. The basic structure of the algorithm is shown in Fig. 2(a).

$X(k)$ is the input of the system at $k$ time, $W(k)$ the weight of the system at $k$ time, $O(k)$ the output of the system at $k$ time, $d(k)$ the target output of the system at $k$ time, and $\varepsilon(k)$ the output error of the system at $k$ time. The minimum mean square error algorithm is adopted for weight adjustment as shown in (17).

$$\begin{cases} \varepsilon(k) = d(k) - O(k) = d(k) - W(k)X(k) \\ W(k+1) = W(k) + 2\eta X(k)\varepsilon(k) \end{cases} \tag{17}$$

where $\eta$ is the weight step factor.

When the ADALINE algorithm shown in Fig. 2(b) and (17) is applied for SPMSM to identify $L_s$, the parameter can be updated according to (18) or (19).

$$\hat{L}_s(k+1) = \hat{L}_s(k) + 2\eta_1 \left[\bar{\omega}_e(k) \cdot \bar{i}_d(k)\right] \left[u_q(k) - \bar{u}_q^*(k)\right] \tag{18}$$

$$\hat{L}_s(k+1) = \hat{L}_s(k) + 2\eta_2 \left[-\bar{\omega}_e(k) \cdot \bar{i}_q(k)\right] \left[u_d(k) - \bar{u}_d^*(k)\right] \tag{19}$$

where $\hat{L}_s$ is the identified inductive value at $k$ time; $[-\bar{\omega}_e(k) \cdot \bar{i}_q(k)]$ and $[\bar{\omega}_e(k) \cdot \bar{i}_d(k)]$ are the input of the ADALINE algorithm at $k$ time; $[u_d(k) - \bar{u}_d(k)]$ and $[u_q(k) - \bar{u}_q(k)]$ are output error in ADALINE algorithm at $k$ time.

$\hat{L}_s$ is corresponding to $W(k)$; $[-\bar{\omega}_e(k) \cdot \bar{i}_q(k)]$ and $[\bar{\omega}_e(k) \cdot \bar{i}_d(k)]$ are corresponding to $X(k)$; $[u_d(k) - \bar{u}_d(k)]$ and $[u_q(k) - \bar{u}_q(k)]$ are corresponding to $\varepsilon(k)$.

According to the parameter update equation, the algorithm structure diagram shown in Fig. 2 is constructed. Figs. 2(c) and 2(d) are combined with (18) and (19), respectively, to update $L_s$.

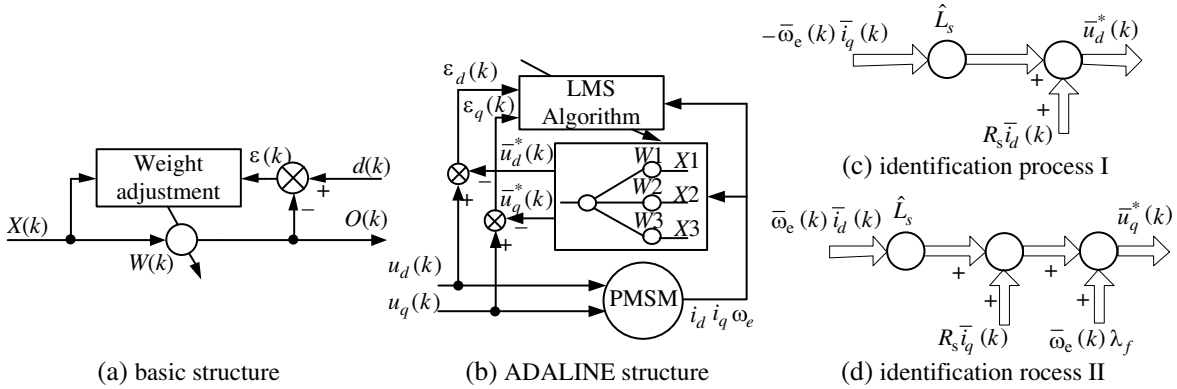


**Figure 2.** Structural block diagram of parameter identification algorithm.

When the algorithm shown in Fig. 2 is used to update $L_s$, it is necessary to limit $\eta$ to satisfy the convergence of the algorithm. Here, weight step factor $\eta$ is constrained by $0 < 2\eta |X(k)|^2 < 1$.

### 3.2. Dead Time Compensation Control Based on ADALINE

According to the previous analysis of DTE, the harmonics order of $d$- and $q$-axis currents is mainly 6 times of the fundamental wave. Therefore, in order to realize DTC control, the harmonic components in $d$- and $q$-axis currents can be filtered directly. Only DC components can be retained, and the filtered $d$- and $q$-axis currents can be transformed into current components in static coordinate system through coordinate transformation for current polarity discrimination [14]. Since the harmonic component in the current is reduced, the occurrence of false compensation can be avoided.

ADALINE algorithm has the ability to adaptively extract harmonic components, so it can be used to extract the 6th harmonics in $d$- and $q$-axis currents, filter them from the original data, and only retain the DC component. The $d$- and $q$-axis currents calculated by ADALINE algorithm are

$$\begin{cases} \hat{i}_d = i_{d0} + i_{d6} = \omega_{d0} + \omega_{d6a} \cos(6\theta_e) + \omega_{d6b} \sin(6\theta_e) \\ \hat{i}_q = i_{q0} + i_{q6} = \omega_{q0} + \omega_{q6a} \cos(6\theta_e) + \omega_{q6b} \sin(6\theta_e) \end{cases} \tag{20}$$

where $i_{d0}$ and $i_{q0}$ are the DC components of $d$- and $q$-axis currents; $i_{d6}$ and $i_{q6}$ are the 6th harmonics of $d$- and $q$-axis currents; $\omega_{d0}$ is the amplitude of DC component; and $\omega_{d6a}$, $\omega_{d6b}$, $\omega_{q6a}$, and $\omega_{q6b}$ respectively represent the amplitudes of the 6th harmonic components of $d$- and $q$-axis currents.

In order to update the current amplitude iteratively, the weight update algorithm needs to be used to adjust it in real time. The simple least mean square algorithm is usually used to update the weight, but the convergence speed of this algorithm is not good. In order to improve the convergence speed of the system, an RLS algorithm with fast convergence speed is proposed to update the weight. The specific formula is

$$\mathbf{V}(k+1) = \mathbf{V}(k) + \mathbf{K}(k) \cdot e(k) \tag{21}$$

where gain $\mathbf{K}(k) = \frac{\mathbf{P}(k-1)\mathbf{X}(k)}{\lambda+\mathbf{X}^{\mathrm{T}}(k)\mathbf{P}(k-1)\mathbf{X}(k)}$, autocorrelation coefficient $\mathbf{P}(k) = \frac{\mathbf{P}(k-1)-\mathbf{K}(k)\mathbf{X}^{\mathrm{T}}(k)\mathbf{P}(k-1)}{\lambda}$, $\lambda$ is the forgetting factor, and the value range is generally set to $0.95 < \lambda < 1$.

The control block diagram of the above algorithm is shown in Fig. 3. According to this algorithm, the 6th harmonic components of $d$- and $q$-axes and the filtered DC components can be obtained. The filtered DC components are transformed into the current component in the static coordinate system after coordinate transformation, and the current components in the static coordinate system are used to judge the current polarity, so as to realize the DTC control. Because the 6th harmonic currents in $d$- and $q$-axes are filtered out by ADALINE algorithm, the DTC effect near zero current is better.

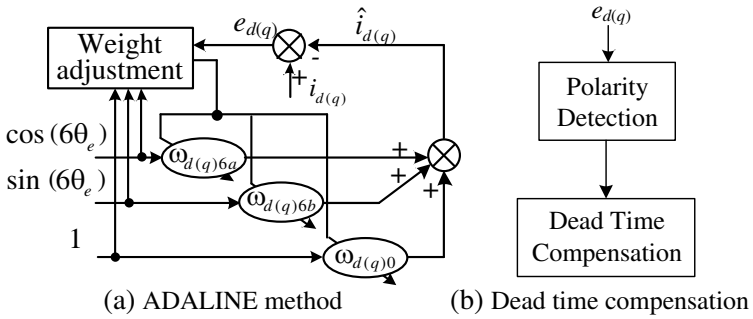


**Figure 3.** Structure block diagram of dead time compensation algorithm.

### 3.3. Overall Structure of the Proposed Control Method

According to the basic formula and theory described above, the block diagram of MPC algorithm of SPMSM based on parameter identification and DTC is shown in the Fig. 4. In the whole control algorithm, the current values at $(k+1)$ moment and $(k+2)$ moment are predicted by sampling current, voltage, speed, and other parameters, and the optimal switching state is selected through the evaluation of cost function. In order to achieve high-performance predictive control effect, it is necessary to obtain the parameter value and dead time state of the system in real time. As can be seen from Fig. 4, the proposed parameter identification algorithm takes current, voltage, and speed as input variables, and the electrical parameter values are obtained after weight updating. Then the identified electrical parameters $R$, $\lambda_f$, and $L_s$ are applied to the current calculation formula (2) and current prediction formula (3). At the same time, $d$- and $q$-axis currents and 6 times electric angle are used as the input of ADALINE algorithm, and the RLS algorithm is used to update the weight and filter the harmonic current. Then the DTC control is realized by coordinate transformation and current polarity discrimination.

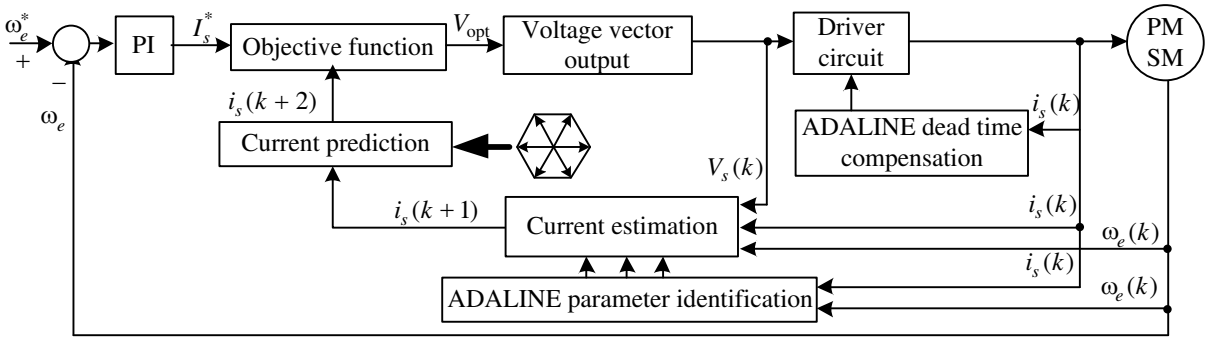


**Figure 4.** Structure block diagram of dead time compensation algorithm.

## 4. EXPERIMENT AND ANALYSIS

In order to verify the effectiveness of this method, the MPC algorithm based on parameter identification and DTC for PMSM is analyzed and verified by experiments. The test bench used in this experiment is shown in Fig. 5. The parameters are shown in Table 1, and the dead time is set to 5 μs.

**Table 1.** Parameters of the prototype.

| Parameters | Value | Parameters | Value |
|---|---|---|---|
| Stator resistance $R$ (Ω) | 1.6 | Rated power $P$ (kW) | 0.2 |
| Stator inductance $L_s$ (H) | 0.005075 | Rated voltage $U$ (V) | 220 |
| Pole Pairs | 4 | Rated current $I$ (A) | 2.1 |
| Permanent magnet flux $\lambda_f$ (Wb) | 0.0825 | Rated torque $T_e$ (N · m) | 0.64 |

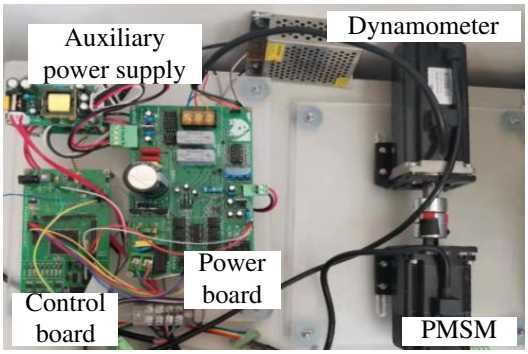


**Figure 5.** Schematic diagram of the experimental platform.

The first is the identification of motor resistance. By injecting $d$-axis current with different amplitudes, the voltage and current at different times and temperatures are obtained. After calculation, the fitting formula $R = 0.00384T + R_0$, where $T$ is the motor temperature, and the unit is °C.

Then the permanent magnet flux linkage is identified. According to the previous analysis, set the $d$-axis current to 0, and collect information such as voltage and current after running the motor to the rated speed. Calculate the flux linkage amplitude according to formula (13). The identification curve of flux linkage amplitude is shown in Fig. 6(a). It can be seen from the figure that the permanent magnet flux finally converges to 0.0823 Wb, which is basically consistent with the amplitude of the permanent magnet flux in the table. Afterwards, the initial value of inductance is identified, and the identification process adopts the method mentioned above. The identification curve of the initial value of inductance is shown in Fig. 6(b). The initial value of inductance finally fluctuates around 5.11 mH, with an error

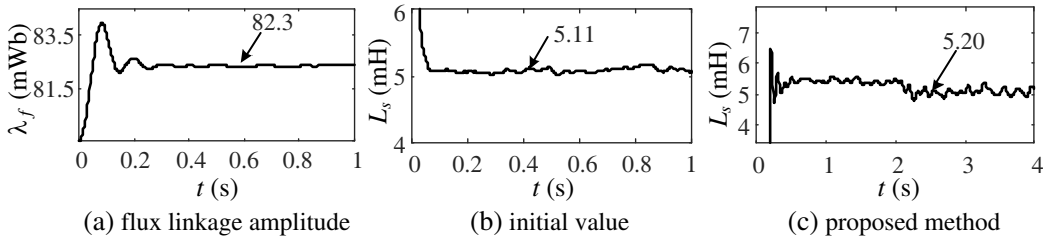


**Figure 6.** Parameters of permanent magnet flux linkage and inductance.

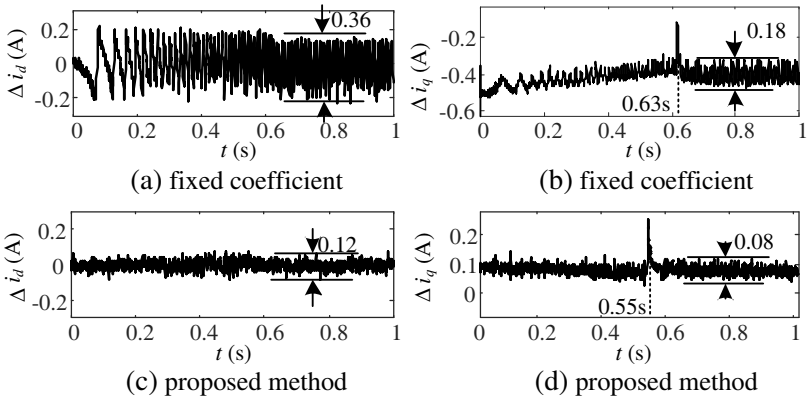


**Figure 7.** Amplitude of error currents.

of 0.69% from the nominal value of 5.075 mH in the table.

When the initial values of resistance, permanent magnet flux linkage, and inductance are identified, these values can be applied to MPC. At the same time, the value of inductance can be adjusted in real time. The identification algorithm adopts the proposed ADALINE method, and the identification results are shown in the Fig. 6(c). It can be seen from the figure that the result of real-time inductance identification fluctuates around 5.20 mH, and the error with the nominal value of 5.075 mH is 2.46%.

In order to verify the effectiveness of the proposed parameter identification algorithm and the influence of the performance of MPC, the identified parameters are applied to the predictive model. Take $d$- and $q$-axis current errors as the index to evaluate the performance. The experimental results are shown in the Fig. 7. It can be seen from the figure that when the parameters are fixed, the errors fluctuations of $d$- and $q$-axis currents are 0.36 A and 0.18 A, respectively. When the parameters are dynamically adjusted by the proposed parameter identification method, the errors fluctuations of $d$- and $q$-axis currents are 0.12 A and 0.08 A, respectively, and the fluctuation amplitudes are reduced by 66.7% and 55.6%, respectively. At the same time, it can be seen from the $q$-axis current error curve that when the parameters are fixed, the speed reaches the given speed in 0.63 s, while when the parameters are changed, the speed reaches the given speed in 0.55 s. Therefore, accurate parameters can not only reduce the current error, but also speed up the dynamic response ability of the speed.

In order to verify the influence of the proposed DTC algorithm on the performance of the control system, the experiments of no DTC and DTC control algorithms are carried out, respectively. The experimental results of no DTC are shown in the Fig. 8(a) and Fig. 8(b). As can be seen from the figures, the fluctuation amplitudes of $d$- and $q$-axis currents are 0.31 A and 0.28 A, respectively, and the amplitudes of the 6th harmonic are 0.012 A and 0.0018 A, respectively. The experimental results of

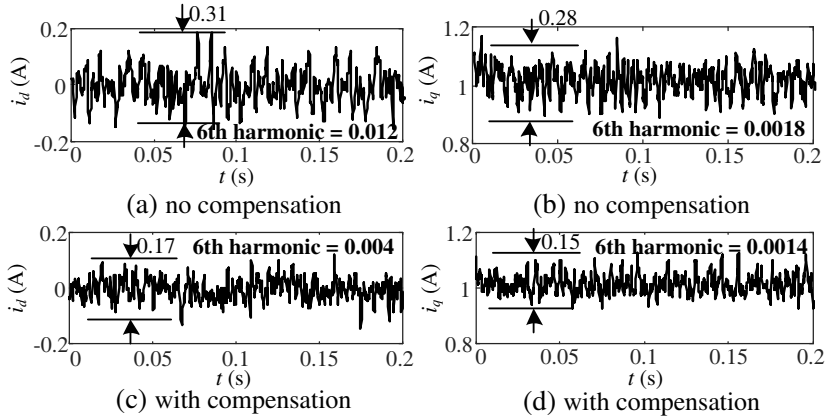


**Figure 8.** Current waveform of dead time compensation control algorithm.

DTC are shown in Fig. 8(c) and Fig. 8(d). After dead time compensation, the fluctuation amplitudes of $d$- and $q$-axis currents are 0.17 A and 0.15 A, respectively, and the amplitudes of the 6th harmonic are 0.004 A and 0.0014 A, respectively. The amplitudes fluctuations of $d$- and $q$-axis currents are reduced by 45.2% and 46.4%, respectively, and the amplitudes of the 6th harmonic are reduced by 66.7% and 22.2%.

In conclusion, after using the proposed parameter identification algorithm and dead time compensation algorithm, the current error and harmonic content of the model predictive control system are effectively suppressed. At the same time, due to the accurate identification of parameters, the dynamic performance of motor speed is greatly improved.

## 5. CONCLUSION

The current control performance of FCS-MPC is sensitive to the parameters of motor model. When the actual parameters do not match the theoretical parameters, the current control performance will be reduced. At the same time, the dead time effect will also cause harmonics in current and voltage, which will reduce the performance of the control system. Therefore, an MPC of PMSM based on parameter identification and dead time compensation is proposed in this paper. The motor parameters are identified in real time by the parameter identification method and applied to the prediction model. At the same time, the harmonic components in the current are quickly filtered by ADALINE method and RLS algorithm, and the dead time compensation control is completed. The experimental results show that this method can effectively suppress the current steady-state error, improve the current control performance, and speed up the dynamic response of speed.

## REFERENCES

1. Sun, Y., Q. Cui, and Y. Yuan, "Research on control of permanent magnet synchronous motor based on second-order sliding mode," *Progress In Electromagnetics Research M*, Vol. 85, 11–20, 2019.
2. Huang, Y., T. Tao, Y. Liu, K. Chen, and F. Yang, "DSC-FLL based sensorless control for permanent magnet synchronous motor," *Progress In Electromagnetics Research M*, Vol. 98, 171–181, 2020.
3. Zhu, L., B. Xu, and H. Zhu, "Interior permanent magnet synchronous motor dead-time compensation combined with extended Kalman and neural network bandpass filter," *Progress In Electromagnetics Research M*, Vol. 98, 193–203, 2020.
4. Liu, X., Y. Pan, Y. Zhu, H. Han, and L. Ji, "Decoupling control of permanent magnet synchronous motor based on parameter identification of fuzzy least square method," *Progress In Electromagnetics Research M*, Vol. 103, 49–60, 2021.
5. Zhu, Y., Y. Bai, H. Wang, and L. Sun, "Sensorless control of permanent magnet synchronous motor based on T-S fuzzy inference algorithm fractional order sliding mode," *Progress In Electromagnetics Research M*, Vol. 105, 161–172, 2021.
6. Fan, M., H. Lin, and T. Lan, "Model predictive direct torque control for spmsm with load angle limitation," *Progress In Electromagnetics Research B*, Vol. 58, 245–256, 2014.
7. Wang, Z., A. Yu, X. Li, G. Zhang, and C. Xia, "A novel current predictive control based on fuzzy algorithm for PMSM," *IEEE Journal of Emerging and Selected Topics in Power Electronics*, Vol. 7, No. 2, 990–1001, Jun. 2019.
8. Zhang, X., L. Zhang, and Y. Zhang, "Model predictive current control for PMSM drives with parameter robustness improvement," *IEEE Transactions on Power Electronics*, Vol. 34, No. 2, 1645–1657, Feb. 2019.
9. Niu, S., Y. Luo, W. Fu, and X. Zhang, "Robust model predictive control for a three-phase PMSM motor with improved control precision," *IEEE Transactions on Industrial Electronics*, Vol. 68, No. 1, 838–849, Jan. 2021.
10. Zhang, Y., J. Jin, and L. Huang, "Model-free predictive current control of PMSM drives based on extended state observer using ultralocal model," *IEEE Transactions on Industrial Electronics*, Vol. 68, No. 2, 993–1003, Feb. 2021.

11. Li, X., W. Tian, X. Gao, Q. Yang, and R. Kennel, "A generalized observer-based robust predictive current control strategy for PMSM drive system," *IEEE Transactions on Industrial Electronics*, Vol. 69, No. 2, 1322–1332, Feb. 2022.
12. Gao, M., H. Zhu, and Y. Shi, "Predictive direct control of permanent magnet assisted bearingless synchronous reluctance motor based on super twisting sliding mode," *Progress In Electromagnetics Research M*, Vol. 102, 105–115, 2021.
13. Zhu, H. and M. Wu, "Direct control of bearingless permanent magnet synchronous motor based on prediction model," *Progress In Electromagnetics Research M*, Vol. 101, 127–138, 2021.
14. Ji, Y., Y. Yong, J Zhou, H. Ding, X. Guo, and S. Padmanaban, "Control strategies of mitigating dead-time effect on power converters: An overview," *Electronics*, Vol. 8, No. 2, 196, 2019.